

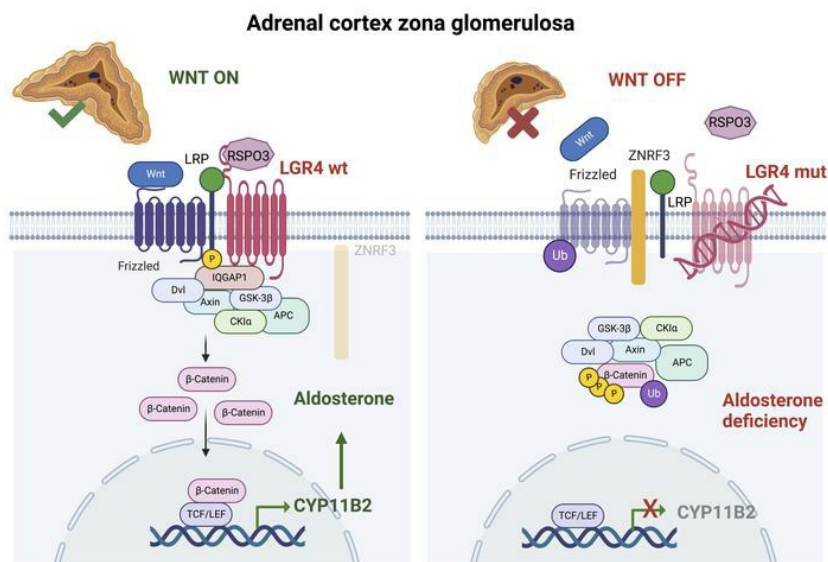
# Loss of LGR4/GPR48 causes severe neonatal salt-wasting due to disrupted WNT signaling altering adrenal zonation

Cécily Lucas, ... , Florence Roucher-Boulez, Christa E. Fluck

*J Clin Invest.* 2022. <https://doi.org/10.1172/JCI164915>.

Research In-Press Preview Endocrinology

## Graphical abstract



Find the latest version:

<https://jci.me/164915/pdf>



1 **Loss of LGR4/GPR48 causes severe neonatal salt-wasting due to disrupted WNT**  
2 **signaling altering adrenal zonation**

3

4 Cécily Lucas<sup>1,2,3\*</sup>, Kay-Sara Sauter<sup>4,5\*</sup>, Michael Steigert<sup>6\*</sup>, Delphine Mallet<sup>1,7</sup>, James Wilmouth<sup>3</sup>,  
5 Julie Olabe<sup>3</sup>, Ingrid Plotton<sup>1,2,7</sup>, Yves Morel<sup>1,2,7</sup>, Daniel Aeberli<sup>8</sup>, Franca Wagner<sup>9</sup>, Hans  
6 Clevers<sup>10</sup>, Amit V. Pandey<sup>4,5</sup>, Pierre Val<sup>3#</sup>, Florence Roucher-Boulez<sup>1,2,3#</sup>, Christa E. Flück<sup>4,5#</sup>

7

8 \* shared first/ # last authors for equal contribution

9 *C.L., K.S.S. and M.S. share the first author position in the given sequence for their specific*  
10 *contribution based on work load and significance to the project (see also list of Authors*  
11 *contribution)*

12

13 <sup>1</sup> Laboratoire de Biochimie et Biologie Moléculaire, UM Pathologies Endocriniennes,  
14 Groupement Hospitalier Est, Hospices Civils de Lyon, Bron, France

15 <sup>2</sup> Univ Lyon, Université Claude Bernard Lyon 1, Lyon, France

16 <sup>3</sup> Université Clermont Auvergne, CNRS, Inserm, GReD, F-63000 Clermont-Ferrand, France

17 <sup>4</sup> Division of Pediatric Endocrinology, Diabetology and Metabolism, Department of Pediatrics,  
18 Inselspital, Bern University Hospital, University of Bern, 3010 Bern, Switzerland

19 <sup>5</sup> Department of Biomedical Research, University of Bern, 3010 Bern, Switzerland

20 <sup>6</sup> Department of Pediatrics, Cantonal Hospital Graubunden, 7000 Chur, Switzerland

21 <sup>7</sup> Centre de Référence Maladies Rares du Développement Génital : du Fœtus à l'Adulte, Filière  
22 Maladies Rares Endocriniennes, Bron, France

23 <sup>8</sup> Department of Rheumatology and Clinical Immunology/Allergology, Inselspital, Bern University  
24 Hospital, University of Bern, 3010 Bern, Switzerland

25 <sup>9</sup> University Institute of Diagnostic and Interventional Neuroradiology, Bern University Hospital,  
26 Inselspital, University of Bern, 3010 Bern, Switzerland

27 <sup>10</sup> Oncode Institute, Hubrecht Institute, Royal Netherlands Academy of Arts and Sciences and  
28 University Medical Centre Utrecht, 3584 CT Utrecht, The Netherlands

29

30 **Corresponding Author:**

31 Christa E. Flück

32 University Children's Hospital Bern

33 Freiburgstrasse 65 / C845

34 3010 Bern

35 Switzerland

36 Phone: +41 31 6320499

37 [christa.flueck@dbmr.unibe.ch](mailto:christa.flueck@dbmr.unibe.ch)

38

39 **Conflict-of-interest statement**

40 The authors have declared that no conflict of interest exists.

41 **ABSTRACT** (199)

42 Disorders of isolated mineralocorticoid deficiency causing potentially life-threatening salt-  
43 wasting crisis early in life have been associated with gene variants of aldosterone biosynthesis  
44 or resistance, but in some patients no such variants are found. WNT/ $\beta$ -catenin signaling is  
45 crucial for differentiation and maintenance of the aldosterone producing adrenal zona  
46 glomerulosa (zG). We describe a highly consanguineous family with multiple perinatal deaths or  
47 infants presenting at birth with failure to thrive, severe salt-wasting crises associated with  
48 isolated hypoaldosteronism, nail anomalies, short stature, and deafness. Whole exome  
49 sequencing revealed a homozygous splice variant in the R-SPONDIN receptor *LGR4* gene  
50 (c.618-1G>C) regulating WNT signaling. The resulting transcripts affected protein function and  
51 stability, and resulted in loss of Wnt/ $\beta$ -catenin signaling *in vitro*. The impact of *LGR4* inactivation  
52 was analyzed by adrenal cortex specific ablation of *Lgr4*, using *Lgr4<sup>Flox/Flox</sup>* mated with *Sf1:Cre*  
53 mice. Inactivation of *Lgr4* within the adrenal cortex in the mouse model caused decreased WNT  
54 signaling, aberrant zonation with deficient zG and reduced aldosterone production. Thus,  
55 human *LGR4* mutations establish a direct link between *LGR4* inactivation and decreased  
56 canonical WNT signaling with abnormal zG differentiation and endocrine function. Therefore,  
57 variants in WNT signaling and its regulators should systematically be considered in familial  
58 hyperreninemic hypoaldosteronism.

59

60 **Key words:**

61 adrenal cortex, human adrenal cortex zonation, zona glomerulosa, mineralocorticoid deficiency,  
62 aldosterone, WNT/ $\beta$ -catenin signaling, *LGR4/GPR 48*, familial hyperreninemic  
63 hypoaldosteronism

## 64 INTRODUCTION

65 Disorders of isolated mineralocorticoid (MC) deficiency are potentially life-threatening (1). So  
66 far, they have been described in humans with primary defects in aldosterone biosynthesis or  
67 with MC resistance due to failure of aldosterone action. Patients mostly manifest in neonatal life  
68 with a salt-wasting crisis, e.g. dehydration, vomiting, and failure to thrive, due to high potassium,  
69 low sodium, metabolic acidosis, and high renin. The disorder becomes usually less severe with  
70 age as physiologic immaturity of the renal tubular system in the first year of life is contributing to  
71 impaired ability to regulate water and sodium homeostasis (2-4), while beyond the neonatal  
72 period a higher sodium intake in the diet regulated by salt appetite centrally may compensate for  
73 MC deficiency (5).

74 In humans, aldosterone is the principal MC produced in the zona glomerulosa (zG) of the  
75 adrenal cortex where the *CYP11B2* gene for aldosterone synthesis is expressed (6).

76 Aldosterone synthesis regulated by the renin-angiotensin-aldosterone (RAA) feedback loop,  
77 controls salt and water homeostasis and blood pressure.

78 Isolated hypoaldosteronism is mostly associated with autosomal recessive variants of the  
79 *CYP11B2* gene, catalyzing aldosterone synthesis. However, a subset of typical cases of  
80 aldosterone deficiency, grouped under Familial Hyperreninemic Hypoaldosteronism (FHHA2)  
81 remains genetically unsolved (1). Mutations in genes that regulate aldosterone biosynthesis,  
82 downstream of renin, including genes encoding angiotensinogen (*AGT*), the angiotensin-  
83 converting enzyme (*ACE*) or the angiotensin II receptor (*AGTR1*) are associated with arterial  
84 hypotension in mice. In humans, these mutations are associated with renal tubular dysgenesis  
85 (7-10). However, they have not been linked with hypoaldosteronism. Other potential candidates  
86 comprise genes involved in the development and differentiation of the adrenal cortex.

87 Adrenal cortex physiology relies on functional zonation, essential for the production of  
88 aldosterone by the outer zG and glucocorticoids by the inner zona fasciculata (zF). The cortex  
89 undergoes constant cell renewal during postnatal life (11). This involves recruitment of

90 subcapsular progenitor cells to zG fate and subsequent conversion to zF identity. This  
91 differentiation occurs in a centripetal manner, under the control of the WNT signaling pathway in  
92 zG and the PKA pathway in zF (12). WNT4 and R-SPONDIN3 (RSPO3) are tissue specific  
93 expressed and thus important drivers of WNT activation and zG differentiation, through  
94 stabilization of  $\beta$ -catenin, which stimulates expression of CYP11B2 and angiotensin II receptor  
95 AGTR1 in the human adrenal cortex (13). Consequently, mouse models with *Ctnnb1*, *Wnt4*, or  
96 *Rspo3* deficiency have reduced zG differentiation(12, 14-16). Conversely, constitutive WNT  
97 pathway activation resulting from activating *CTNNB1* mutations or downregulation of negative  
98 WNT regulators is associated with the development of aldosterone-producing adenomas (17,  
99 18). Despite the central role of canonical WNT signaling in zG differentiation, mutations in this  
100 pathway have not been associated with hypoaldosteronism in humans so far. Here, we  
101 identified a loss of function splice variant of the R-SPONDIN receptor coding *LGR4* gene (c.618-  
102 1G>C) in a girl born into a highly consanguineous family with a history of multiple perinatal  
103 deaths. The proband presented with failure to thrive, severe salt-wasting crises associated with  
104 isolated hypoaldosteronism, nail anomalies, short stature, and deafness. Our *in silico*, *in vitro*  
105 and *in vivo* studies establish a causal link between LGR4 inactivation, decreased canonical  
106 WNT signaling, abnormal zG differentiation and endocrine function. This suggests that  
107 anomalies in WNT signaling pathway regulators should systematically be evaluated in familial  
108 hyperreninemic hypoaldosteronism.

109

## 110 **RESULTS**

111 In a highly consanguineous family from Syria, newborns were found to suffer from salt-wasting  
112 crises soon after birth due to isolated aldosterone deficiency. In addition, they revealed a  
113 common syndromic phenotype of nail dysplasia, deafness, growth restriction, and mental  
114 disability. The index patient was referred at the age of 17 years for adrenal insufficiency, short  
115 stature, deafness, developmental delay, and dysplastic nails (Figure 1 and Suppl Figure S1).

116 She was born at term and manifested within days, with failure to thrive and signs of an adrenal  
117 salt-wasting crisis. Corticosteroid treatment was successfully installed without further  
118 investigations. Parents are first-degree cousins from Syria. The presence of the same  
119 phenotype in 3 siblings deceased in the neonatal period, and two cousins (with consanguineous  
120 parents) was indicative of an autosomal recessive disorder. Laboratory workup revealed normal  
121 cortisol response to ACTH stimulation, but hyperreninemic hypoaldosteronism (Table 1). Thus  
122 the diagnosis was revised to isolated mineralocorticoid deficiency and therapy continued with  
123 fludrocortisone, while genetic workup was initiated. Additional important findings were short  
124 stature, microcephaly, structural brain anomalies, and mental disability; deafness with functional  
125 but without structural anomalies of the cochlea and hearing nerve; low bone mineral density,  
126 and small kidneys with cortical microlesions (Suppl Figures S1-4 and Table S1). Pubertal  
127 development was late with menarche at 16 years.

128 Of note, two cousins with the same clinical phenotype (one female and one male) are alive  
129 under steroid replacement therapy in Syria but are not available for investigations. A detailed  
130 description of the clinical findings is given in the Supplementary Appendix.

131

### 132 ***Identification of a human LGR4 variant***

133 After exclusion of *CYP11B2* mutations, filtering of the exome sequences identified a  
134 homozygous mutation in the proband *LGR4* gene: NM\_018490:c.618-1G>C. Both parents and  
135 one brother were heterozygous for the same *LGR4* mutation but showed no overt phenotype  
136 (Figure 1B; Suppl Table S2). The variant affects a splicing acceptor site, predicted to result in  
137 exon 6 skipping, and deletion r.618\_689del or p.(His207\_Leu230del). mRNA transcript analysis  
138 of patient's fibroblasts confirmed exon 6 skipping, but also identified a second transcript with an  
139 alternative acceptor site within exon 6, leading to a shorter deletion of -24 bp, r.618\_641del or  
140 p.(His207\_Arg214) (Figure 1C).

141

142 ***In silico analysis of LGR4 variants for prediction of pathogenicity***

143 Leucine-rich repeat-containing G-protein-coupled receptors (LGR) are characterized by  
144 Leucine-Rich Repeats (LRRs) that provide the rigid structure of their large extracellular domain.  
145 LGR4 is a receptor for R-SPONDINS (RSPOs). The binding of RSPOs to LGR4 stimulates  
146 Wnt/ $\beta$ -catenin signaling pathway by inhibiting the E3-ubiquitin ligases ZNRF3/RNF43 (19).  
147 RSPOs bind to the first LRR and LRR3-LRR9 (20). The amino acid deletions caused by the loss  
148 of 8 and 24 amino acids in LGR4 are located in LRR7 and 8, in the extracellular domain of  
149 LGR4 (Figure 1D). A protein sequence alignment of LGR4 across species revealed that  
150 sections of LGR4 that comprise LRR7 and LRR8 are highly conserved (Suppl Figure S5).  
151 Regions of RSPOs that interact with LGR4 are conserved among RSPOs isoforms (Suppl  
152 Figure S6) and across species (Suppl Figure S7). Mutations in the patient resulted in the  
153 deletion of parts of the LGR4 protein in its extracellular domain within LRR7 (for -8AA variant)  
154 and LRR7 and LRR8 (for -24AA variant). Structural analysis of contacts between LGR4 and  
155 RSPO1/RSPO3 showed that multiple contact points between the two proteins in the complex  
156 are located in LRR7 and LRR8 (Val204, His207, Asn226, Thr229, Tyr234 and Glu252) (Suppl  
157 Figure S8). A loss of multiple contact points due to the deletions would result in significantly  
158 weaker interaction between LGR4 and RSPOs and impact the overall structures of complexes  
159 involving other interaction partners (ZNRF3, RNF43, UBB, UBC etc). In addition, the deletions  
160 were predicted to result in loss of protein stability and decreased half-life, which could alter  
161 LGR4 protein expression levels in the patients. Together with weaker complex formation, lower  
162 protein levels should result in an overall loss of interaction of the -8AA and -24AA variants of  
163 LGR4 found in patients, with the -24AA variant predicted to have a higher impact.

164

165 ***Analysis of LGR4 protein expression in human fibroblasts***

166 Western blot analysis showed that patient fibroblasts expressed LGR4 protein minimally  
167 compared to controls (Figure 2A), but the expression was also low in control fibroblasts from



168 healthy individuals. Unfortunately, biomaterial from heterozygote family members was not  
169 available.

170

### 171 ***Functional analysis of LGR4 variants in cell models***

172 To assess the function of identified LGR4 variants on RSPO1 activated Wnt signaling, we used  
173 an established TOP-Flash luciferase reporter assay (21-26). When using fibroblasts, RSPO1  
174 stimulation of endogenous LGR4 – Wnt/  $\beta$ -catenin signaling was not strong enough for  
175 luciferase readout. Therefore, we performed the studies in HEK293T cells that were transiently  
176 transfected with wild-type and variants of LGR4. While the basal activity of the Wnt/ $\beta$ -catenin  
177 signaling was low and did not differ between wild-type and LGR4 variants, RSPO1 activated  
178 signaling was increased 6.1-fold with WT-LGR4 ( $p < 0.0001$ , Figure 2B). By contrast, the LGR4  
179 nt-24 variant increased the Wnt/ $\beta$ -catenin signaling only 3.3.-fold ( $p < 0.0001$ ), and the LGR4 nt-  
180 72 variant completely failed to activate Wnt/ $\beta$ -catenin signaling (Figure 2B). Thus, compared to  
181 WT, the LGR4 nt-72 showed loss of function, while the LGR4 variant nt -24 had 54% activity. In  
182 line with these results, loss of interaction by deletion of 24 amino acids in the nt-72 variant was  
183 predicted to have a higher impact on the binding as well as protein stability (Suppl Figure S8),  
184 which explains the very low level of LGR4 protein detected in western blots of patient  
185 fibroblasts.

186

### 187 ***Analysis of localization of LGR4 and binding to RSPO1 in HEK293 cells***

188 LGR4 localizes to the cell membrane and reveals its signal-transducing functionality upon  
189 binding to R-SPONDINS (21-27). To assess localization and RSPO1 binding characteristics of  
190 wild-type and mutant LGR4 proteins, we expressed HA-tagged LGR4 in HEK293 cells and  
191 studied its binding to GFP-tagged RSPO1 by confocal microscopy. As depicted in Figure 2C,  
192 LGR4 localized to the cell surface. nt-24-LGR4 was expressed at a lower level than WT-LGR4,  
193 and cells carrying the nt-72-LGR4 expressed the lowest level of LGR4 (Figure 2D), in line with

194 LGR4 protein expression in patient fibroblasts (Figure 2A). RSPO1 binding with LGR4 protein  
195 was also altered with nt-24-LGR4 compared to wild-type, and almost absent with nt-72 (Figure 2  
196 C,D). Altogether, these *in vitro* data show that the mutant LGR4 proteins identified in the  
197 proband are deficient in their ability to bind R-SPONDINS and stimulate downstream WNT  
198 signaling.

199

### 200 ***Lgr4* ablation results in disrupted *Wnt/β-catenin* signaling pathway in mice**

201 To study the role of LGR4 in adrenal function *in vivo*, we conditionally inactivated *Lgr4* within  
202 steroidogenic cells in the adrenal cortex of *Lgr4*cKO mice. RTqPCR showed a reduction in *Lgr4*  
203 mRNA, confirming efficient deletion of the floxed allele in *Lgr4*cKO mice (Suppl Figure S9A).  
204 Consistent with our *in vitro* data, conditional inactivation of *Lgr4* resulted in a significant  
205 decrease in expression of WNT target genes in the adrenals of *Lgr4*cKO mice (*Apcdd1*, *Axin2*,  
206 and *Lef1*) (Figure 3A) with decreased accumulation of both β-Catenin and LEF1 proteins in the  
207 presumptive zG of mutant mice, where they normally accumulate in control mice (Figure 3B-C).

208

### 209 ***Lgr4* ablation causes adrenal hypoplasia and aberrant zonal differentiation**

210 The reduced canonical WNT signaling in *Lgr4*cKO mice was associated with decreased adrenal  
211 weight at 5 weeks (Figure 3D), massive cortical thinning, off-center localization of the adrenal  
212 medulla, steroidogenic cell cytomegaly, and a significant decrease in cortical cells numbers  
213 (Figure 3E-F). Interestingly, adrenal cortex thinning was not associated with decreased  
214 proliferation or increased apoptosis, suggesting that it relied on altered  
215 development/maintenance of the gland (Suppl Figure S9B-C). Analysis of adrenal cortex  
216 differentiation by immunohistochemistry showed a marked decrease in the number of cells  
217 expressing the zG marker DAB2 and expansion of the expression domain of zF marker  
218 AKR1B7 up to the capsule, where the zG normally resides (Figure 3G). *Lgr4* deficiency also  
219 resulted in the accumulation of cells with both zG (DAB2+) and zF (AKR1B7+) identity that were

220 not found in control mice (Figure 3G, arrowheads), demonstrating a marked impairment of  
221 adrenal cortex differentiation. Aberrant cortical differentiation was further confirmed by RTqPCR  
222 showing increased *Akr1b7* (zF) and decreased expression of the zG markers *Dab2* and *Hsd3b6*  
223 (Figure 3H), consistent with previous data showing decreased zG differentiation and expansion  
224 of zF in mice with decreased adrenal WNT signaling (12, 15).

225

### 226 ***Lgr4* ablation inhibits zG zonation resulting in primary hypoaldosteronism**

227 Consistent with observations in our patient, zG differentiation anomalies in *Lgr4*cKO mice  
228 resulted in a significant decrease in plasma aldosterone (Figure 4A) and an increase in  
229 hematocrit, suggestive of dehydration (Figure S9C). The observation of normal plasma renin  
230 activity (Figure 4B) suggested that hypoaldosteronism in *Lgr4*cKO mice was of primary adrenal  
231 origin. This was further supported by the almost complete extinction of CYP11B2 protein  
232 expression in the *Lgr4*cKO zG (Figure 4C-D). Interestingly, plasma corticosterone concentration  
233 was significantly decreased (Figure 4E), which was associated with a significant decrease in  
234 *Cyp11a1* expression, which is essential for the first step of both aldosterone and corticosterone  
235 synthesis (Figure 4G). However, there was a concomitant increase in *Cyp21* and *Cyp11b1*  
236 expression, which was not associated with altered plasma ACTH concentration (Figure 4F-G).  
237 This may reflect the aberrant expansion of zF at the expense of zG, and hence an increased  
238 ratio of zF to zG cells, rather than a direct effect of ACTH on steroidogenic gene expression.  
239 Altogether, these data show that *Lgr4* inactivation is sufficient to significantly reduce WNT  
240 signaling in the adrenal cortex, which results in early-onset primary hypoaldosteronism.

241

242

### 243 **DISCUSSION**

244 Although adrenal insufficiency with MC and GC deficiencies has been reported for several  
245 complex syndromes where genetic variants lead to structural and/or functional defects of the

246 adrenals and other organ systems (e.g. IMAGE, MIRAGE syndromes) (11), an inherited  
247 syndrome with isolated MC deficiency at birth, has not been described so far. In this study, we  
248 identified a novel syndromic form of severe neonatal salt-wasting in a highly consanguineous  
249 family. In the index patient, isolated mineralocorticoid deficiency was diagnosed and treated  
250 successfully with mineralocorticoid replacement therapy, while cortisol production remained  
251 normal in the first two decades of life. Associated defects included nail anomalies, hearing loss,  
252 short stature, and mental disability in the index patient and both affected cousins (Figure 1A).  
253 We were aided by the consanguinity in this family to reveal the underlying genetic cause,  
254 involving a homozygous splice site variation in the *LGR4* gene (ch11p14.1) producing two  
255 shorter splice variants. *LGR4*, also named GPR48, is a leucine-rich repeat-containing G-protein  
256 coupled receptor, widely expressed in multiple tissues from early embryogenesis to adulthood  
257 (19, 28). *LGR4* potentiates canonical WNT signaling, through inhibition of the ZNRF3/RNF43-  
258 mediated degradation of Frizzled receptors, after binding to R-SPONDINS (19). Consistent with  
259 this, our *in vitro* studies showed that the two aberrant *LGR4* transcripts found in the proband,  
260 coded for proteins with significantly reduced activity on WNT/ $\beta$  catenin signaling *in vitro*. We  
261 further showed that genetic inactivation of *Lgr4* within steroidogenic cells of the adrenal cortex  
262 of transgenic mice resulted in decreased canonical WNT signaling, deficient zG differentiation,  
263 and reduced aldosterone production. Even though previous reports had shown adrenal  
264 dysgenesis in patients with inactivating mutations of *WNT4* in the context of SERKAL syndrome,  
265 profound developmental defects resulted in embryonic lethality, precluding evaluation of adrenal  
266 differentiation and endocrine activity (29). Therefore, to the best of our knowledge, our study is  
267 the first to demonstrate a key role of *LGR4* and more broadly of deficient canonical WNT  
268 signaling in adrenal differentiation and zG hypofunction in patients.

269

270 Beyond primary hypoaldosteronism, the index case also presented with a spectrum of defects  
271 including nail anomalies, hearing loss, and short stature, which were also associated with *in*

272 *utero* death of presumably affected siblings. Our model of conditional *Lgr4* ablation within  
273 steroidogenic cells did not allow evaluation of LGR4 in these phenomena. However, studies of  
274 LGR4 variants in patients and of whole-body *Lgr4* knockout mice demonstrated the association  
275 between LGR4 alterations and fetal/ perinatal death, short stature, deafness, and dysplastic  
276 nails (Supplementary Table S3). This strongly suggests that the broad defects observed in our  
277 proband are the result of the identified LGR4 mutation. So far only individuals who carry  
278 heterozygous LGR4 variants were described. Heterozygous human LGR4 variants are  
279 associated with low bone mineral density, electrolyte imbalance, reduced testosterone  
280 production, and increased risk of cancers of the biliary system and skin (30). More recently, 3  
281 rare heterozygous missense variants in *LGR4* were associated with delayed puberty, resulting  
282 from alterations in the development of hypothalamic GnRH neurons (31). In line with these  
283 findings, heterozygous family members as well as our index patient had delayed pubertal onset  
284 and low bone mineral density (Suppl Appendix Extended Case Report, Figure S4 and Suppl  
285 Table S1 and S3).

286 Loss of LGR4 is also potentially implicated in the rare aniridia-genitourinary anomalies-mental  
287 retardation (AGR) syndrome, where a heterozygous, contiguous gene deletion of the 11p13-14  
288 region had been identified comprising the *LGR4* gene. Similar to the phenotype of AGR  
289 syndrome, whole-body deletion of *Lgr4* in mouse led to aniridia, polycystic kidney disease,  
290 genitourinary anomalies, and mental retardation (32). Although there were no reports of adrenal  
291 dysfunction in these cases, our results suggest that patients presenting with homozygous  
292 LGR4-associated genetic variations should be carefully evaluated for adrenal function.

293

294 Whereas *Lgr4*cKO mice show defects in both aldosterone and corticosterone secretion as early  
295 as 5 weeks, our index case presented with isolated mineralocorticoid deficiency in the first two  
296 decades of life. This phenotypic discrepancy could be accounted for by the residual activity of  
297 mutant LGR4 proteins in our patient, compared with the complete inactivation of LGR4 in the

298 adrenal cortex of our transgenic model. However, ACTH stimulation testing of our patient at 21  
299 years, showed subclinical glucocorticoid deficiency. This suggests that the endocrine phenotype  
300 may progress towards full-fledged adrenal deficiency over time. Lineage tracing studies in mice  
301 have shown that adrenal cortex cell renewal requires initial differentiation of progenitors into zG  
302 cells that subsequently differentiate into zF cells (33, 34). It is thus tempting to speculate that  
303 aberrant zG differentiation in our patient hampered cortical cell renewal, resulting in progressive  
304 exhaustion of the zF, associated with progressive glucocorticoid insufficiency. This warrants  
305 careful monitoring of patients initially presenting with primary hypoaldosteronism, without  
306 *CYP11B2* inactivating mutations.

307

308 In conclusion, we describe the first patients harboring biallelic *LGR4* variants and offer the  
309 mechanistic explanation for their life-threatening salt loss at birth, due to primary adrenal  
310 hypoaldosteronism. Our study confirms the important role of Wnt/ $\beta$ -catenin signaling for proper  
311 adrenal cortex zG and zF formation and function. Thus *LGR4* variants and potential variants in  
312 other genes involved in the complex network of LGR4-Wnt/ $\beta$ -catenin signaling should be  
313 considered in patients presenting with a salt-wasting crisis at birth, especially when manifesting  
314 with other syndromic features.

315

## 316 **METHODS**

### 317 ***Genomic sequencing***

318 We sequenced the exome of the affected child, her parents, and her two unaffected brothers.  
319 Details are provided in Supplementary Appendix. Next-generation sequencing data have been  
320 deposited in the European Genome-phenome Archive (EGA), which is hosted by the EBI and  
321 the CRG, under accession number EGAS00001006808 (<https://ega-archive.org>).

322

### 323 ***Bioinformatic and laboratory studies***

324 Primary fibroblasts of skin biopsies from the proband and healthy controls permitted *LGR4*  
325 transcript analysis and studies of protein expression. The putative impact of the specific *LGR4*  
326 variants was analyzed *in silico* using the three-dimensional structure of the human *LGR4*  
327 extracellular domain in complex with a part of R-SPONDIN (PDB # 4KT1). The function of  
328 identified *LGR4* variants was analyzed *in vitro*, using the TOP-Flash WNT signaling luciferase  
329 reporter assay in the presence or absence of RSPO1. Localization of mutant *LGR4* and  
330 interaction with RSPO1 was investigated by confocal microscopy in HEK293 cells expressing  
331 HA-tagged *LGR4* and GFP-tagged RSPO1. The impact of *LGR4* inactivation *in vivo* was  
332 analyzed by adrenal cortex specific ablation of *Lgr4*, using *Lgr4<sup>Flox/Flox</sup>* mice mated with *Sf1:Cre*  
333 mice. Full experimental details are provided in the Supplementary Appendix.

334

### 335 **Statistics**

336 Results are presented as means +/- SEM. The D'agostino and Pearson normality test  
337 demonstrated the absence of normality of the data. Therefore, statistical analyses between two  
338 or several groups were performed using Mann-Whitney or Kruskal-Wallis, respectively, using  
339 GraphPad Prism 9. A *P* value below 0.05 was considered statistically significant. \**P*<0.05;  
340 \*\**P*<0.01; \*\*\**P*<0.001, \*\*\*\**P*<0.00001.

341

### 342 **Study Approval**

343 Written informed consent was obtained from all subjects. Studies in humans or on human  
344 material were conducted in accordance with Swissethics, Switzerland (KEK Bern ID 04/07).  
345 Animal experiments were approved by the Auvergne ethics committee (CEMEAA), France  
346 (APAFIS #39127).

347

### 348 **Author Contributions**

349 C.L. - Performed experiments on mice biomaterials. Analyzed data. Created Figures.  
350 Contribution to manuscript writing; [cecily.lucas6@gmail.com](mailto:cecily.lucas6@gmail.com)  
351 K.S.S. – Performed experiments on human biomaterials. Analyzed data. Created Figures.  
352 Contribution to manuscript writing; [kay.sauter@dbmr.unibe.ch](mailto:kay.sauter@dbmr.unibe.ch)  
353 M.S. – Clinical workup of the patient. Contribution to manuscript writing and reviewing;  
354 [michael.steigert@ksgr.ch](mailto:michael.steigert@ksgr.ch)  
355 D.M. – Performed genetic test and analysis. Contribution to manuscript writing.  
356 [delphine.mallet@chu-lyon.fr](mailto:delphine.mallet@chu-lyon.fr)  
357 A.V.P. – Bioinformatic analyses and predictions. Created Figures. Contribution to manuscript  
358 writing and reviewing; [amit@pandeylab.org](mailto:amit@pandeylab.org)  
359 J.W. - Performed experiments on mice biomaterials. [jwilmouth21@gmail.com](mailto:jwilmouth21@gmail.com)  
360 J.O. - Performed experiments on mice biomaterials. [julie.olabe@gmail.com](mailto:julie.olabe@gmail.com)  
361 I.P. – Performed hormonal tests. [ingrid.plotton@chu-lyon.fr](mailto:ingrid.plotton@chu-lyon.fr)  
362 Y.M. - Performed genetic test and analysis. [yvmor2@gmail.com](mailto:yvmor2@gmail.com)  
363 D.A. – Clinical workup of patient (bone phenotype), manuscript review; [daniel.aeberli@insel.ch](mailto:daniel.aeberli@insel.ch)  
364 F.W. - Clinical workup of patient (brain, cochlea phenotype); manuscript review;  
365 [franca.wagner@insel.ch](mailto:franca.wagner@insel.ch)  
366 H.C. – Mouse model; [h.clevers@hubrecht.eu](mailto:h.clevers@hubrecht.eu)  
367 P.V. - Study PI. Overall design, organization, data analysis and interpretation. Manuscript  
368 writing. [pierre.val@uca.fr](mailto:pierre.val@uca.fr)  
369 F.R.B. - Study PI. Overall design, organization, data analysis and interpretation. Manuscript  
370 writing. [florence.roucher@chu-lyon.fr](mailto:florence.roucher@chu-lyon.fr)  
371 C.E.F. – Study PI. Overall design, organization, data analysis and interpretation. Manuscript  
372 writing; corresponding author. [christa.flueck@dbmr.unibe.ch](mailto:christa.flueck@dbmr.unibe.ch)

373

374 **Acknowledgments**



375 We thank the patient and family for participating in the study. We acknowledge the help of  
376 Christelle Damon-Soubeyrand and the Anipath histopathology facility (iGReD), Clermont-  
377 Ferrand, for mouse tissue analyses. We also thank Khirredine Ouchen, Sandrine Plantade and  
378 Philippe Mazuel for animal care.

379 Funding: Pierre Val is supported by a program grant (Labellisation) by the “Ligue Nationale  
380 Contre le Cancer” 2021-2025. Florence Roucher-Boulez is supported by the Endocrinology  
381 Research Grant RECORDATI Rare Diseases of the French Society of Endocrinology (SFE)  
382 2020 and the Young Researchers 2021 grant by the Lyon University Hospital (HCL). This work  
383 has also been supported by the Swiss National Science Foundation grant ID 320030\_146127 to  
384 Christa E. Flück. Authors confirm that the study sponsors played no role in study design, data  
385 collection, analysis, and interpretation of data; they were also not involved in the writing of the  
386 report and in the decision to submit the paper for publication.

387 **References**

- 388 1. Miller WL, Fluck CE, Breault DT, and Feldman BJ. In: Sperling MA ed. *Sperling -*  
389 *Pediatric Endocrinology*. Elsevier; 2020.
- 390 2. Holtback U, and Aperia AC. Molecular determinants of sodium and water balance during  
391 early human development. *Semin Neonatol*. 2003;8(4):291-9.
- 392 3. Martinerie L, Pussard E, Foix-L'Helias L, Petit F, Cosson C, Boileau P, et al.  
393 Physiological partial aldosterone resistance in human newborns. *Pediatr Res*.  
394 2009;66(3):323-8.
- 395 4. Rosler A. The natural history of salt-wasting disorders of adrenal and renal origin. *J Clin*  
396 *Endocrinol Metab*. 1984;59(4):689-700.
- 397 5. Fu Y, and Vallon V. Mineralocorticoid-induced sodium appetite and renal salt retention:  
398 evidence for common signaling and effector mechanisms. *Nephron Physiol*. 2014;128(1-  
399 2):8-16.
- 400 6. Miller WL, and Auchus RJ. The molecular biology, biochemistry, and physiology of  
401 human steroidogenesis and its disorders. *Endocr Rev*. 2011;32(1):81-151.
- 402 7. Krege JH, John SW, Langenbach LL, Hodgin JB, Hagaman JR, Bachman ES, et al.  
403 Male-female differences in fertility and blood pressure in ACE-deficient mice. *Nature*.  
404 1995;375(6527):146-8.
- 405 8. Tanimoto K, Sugiyama F, Goto Y, Ishida J, Takimoto E, Yagami K, et al.  
406 Angiotensinogen-deficient mice with hypotension. *J Biol Chem*. 1994;269(50):31334-7.
- 407 9. Sugaya T, Nishimatsu S, Tanimoto K, Takimoto E, Yamagishi T, Imamura K, et al.  
408 Angiotensin II type 1a receptor-deficient mice with hypotension and hyperreninemia. *J*  
409 *Biol Chem*. 1995;270(32):18719-22.
- 410 10. Gribouval O, Gonzales M, Neuhaus T, Aziza J, Bieth E, Laurent N, et al. Mutations in  
411 genes in the renin-angiotensin system are associated with autosomal recessive renal  
412 tubular dysgenesis. *Nature genetics*. 2005;37(9):964-8.
- 413 11. Pignatti E, and Fluck CE. Adrenal cortex development and related disorders leading to  
414 adrenal insufficiency. *Molecular and cellular endocrinology*. 2021;527:111206.
- 415 12. Drelon C, Berthon A, Sahut-Barnola I, Mathieu M, Dumontet T, Rodriguez S, et al. PKA  
416 inhibits WNT signalling in adrenal cortex zonation and prevents malignant tumour  
417 development. *Nat Commun*. 2016;7:12751.
- 418 13. Berthon A, Drelon C, Ragazzon B, Boulkroun S, Tissier F, Amar L, et al. WNT/beta-  
419 catenin signalling is activated in aldosterone-producing adenomas and controls  
420 aldosterone production. *Human molecular genetics*. 2014;23(4):889-905.
- 421 14. Heikkila M, Peltoketo H, Leppaluoto J, Ilves M, Vuolteenaho O, and Vainio S. Wnt-4  
422 deficiency alters mouse adrenal cortex function, reducing aldosterone production.  
423 *Endocrinology*. 2002;143(11):4358-65.
- 424 15. Vidal V, Sacco S, Rocha AS, da Silva F, Panzolini C, Dumontet T, et al. The adrenal  
425 capsule is a signaling center controlling cell renewal and zonation through Rspo3.  
426 *Genes & development*. 2016;30(12):1389-94.
- 427 16. Leng S, Pignatti E, Khetani RS, Shah MS, Xu S, Miao J, et al. beta-Catenin and FGFR2  
428 regulate postnatal rosette-based adrenocortical morphogenesis. *Nat Commun*.  
429 2020;11(1):1680.
- 430 17. Boulkroun S, Samson-Couterie B, Golib-Dzib JF, Amar L, Plouin PF, Sibony M, et al.  
431 Aldosterone-producing adenoma formation in the adrenal cortex involves expression of  
432 stem/progenitor cell markers. *Endocrinology*. 2011;152(12):4753-63.
- 433 18. Berthon A, Sahut-Barnola I, Lambert-Langlais S, de Joussineau C, Damon-Soubeyrand  
434 C, Louiset E, et al. Constitutive beta-catenin activation induces adrenal hyperplasia and  
435 promotes adrenal cancer development. *Human molecular genetics*. 2010;19(8):1561-76.

- 436 19. Ordaz-Ramos A, Rosales-Gallegos VH, Melendez-Zajgla J, Maldonado V, and Vazquez-  
437 Santillan K. The Role of LGR4 (GPR48) in Normal and Cancer Processes. *Int J Mol Sci.*  
438 2021;22(9).
- 439 20. Petrie EJ, Lagaida S, Sethi A, Bathgate RA, and Gooley PR. In a Class of Their Own -  
440 RXFP1 and RXFP2 are Unique Members of the LGR Family. *Front Endocrinol*  
441 *(Lausanne)*. 2015;6:137.
- 442 21. Carmon KS, Gong X, Lin Q, Thomas A, and Liu Q. R-spondins function as ligands of the  
443 orphan receptors LGR4 and LGR5 to regulate Wnt/beta-catenin signaling. *Proc Natl*  
444 *Acad Sci U S A*. 2011;108(28):11452-7.
- 445 22. Glinka A, Dolde C, Kirsch N, Huang YL, Kazanskaya O, Ingelfinger D, et al. LGR4 and  
446 LGR5 are R-spondin receptors mediating Wnt/beta-catenin and Wnt/PCP signalling.  
447 *EMBO Rep*. 2011;12(10):1055-61.
- 448 23. Korinek V, Barker N, Morin PJ, van Wichen D, de Weger R, Kinzler KW, et al.  
449 Constitutive transcriptional activation by a beta-catenin-Tcf complex in APC<sup>-/-</sup> colon  
450 carcinoma. *Science*. 1997;275(5307):1784-7.
- 451 24. Ruffner H, Sprunger J, Charlat O, Leighton-Davies J, Grosshans B, Salathe A, et al. R-  
452 Spondin potentiates Wnt/beta-catenin signaling through orphan receptors LGR4 and  
453 LGR5. *PLoS One*. 2012;7(7):e40976.
- 454 25. Tomaselli S, Megiorni F, Lin L, Mazzilli MC, Gerrelli D, Majore S, et al. Human  
455 RSPO1/R-spondin1 is expressed during early ovary development and augments beta-  
456 catenin signaling. *PLoS One*. 2011;6(1):e16366.
- 457 26. de Lau W, Barker N, Low TY, Koo BK, Li VS, Teunissen H, et al. Lgr5 homologues  
458 associate with Wnt receptors and mediate R-spondin signalling. *Nature*.  
459 2011;476(7360):293-7.
- 460 27. Kudo M, Chen T, Nakabayashi K, Hsu SY, and Hsueh AJ. The nematode leucine-rich  
461 repeat-containing, G protein-coupled receptor (LGR) protein homologous to vertebrate  
462 gonadotropin and thyrotropin receptors is constitutively active in mammalian cells.  
463 *Molecular endocrinology*. 2000;14(2):272-84.
- 464 28. Yi J, Xiong W, Gong X, Bellister S, Ellis LM, and Liu Q. Analysis of LGR4 receptor  
465 distribution in human and mouse tissues. *PLoS One*. 2013;8(10):e78144.
- 466 29. Mandel H, Shemer R, Borochoy ZU, Okopnik M, Knopf C, Indelman M, et al. SERKAL  
467 syndrome: an autosomal-recessive disorder caused by a loss-of-function mutation in  
468 WNT4. *American journal of human genetics*. 2008;82(1):39-47.
- 469 30. Styrkarsdottir U, Thorleifsson G, Sulem P, Gudbjartsson DF, Sigurdsson A, Jonasdottir  
470 A, et al. Nonsense mutation in the LGR4 gene is associated with several human  
471 diseases and other traits. *Nature*. 2013;497(7450):517-20.
- 472 31. Mancini A, Howard SR, Marelli F, Cabrera CP, Barnes MR, Sternberg MJ, et al. LGR4  
473 deficiency results in delayed puberty through impaired Wnt/beta-catenin signaling. *JCI*  
474 *Insight*. 2020;5(11).
- 475 32. Yi T, Weng J, Siwko S, Luo J, Li D, and Liu M. LGR4/GPR48 inactivation leads to  
476 aniridia-genitourinary anomalies-mental retardation syndrome defects. *J Biol Chem*.  
477 2014;289(13):8767-80.
- 478 33. Freedman BD, Kempna PB, Carlone DL, Shah M, Guagliardo NA, Barrett PQ, et al.  
479 Adrenocortical zonation results from lineage conversion of differentiated zona  
480 glomerulosa cells. *Dev Cell*. 2013;26(6):666-73.
- 481 34. King P, Paul A, and Laufer E. Shh signaling regulates adrenocortical development and  
482 identifies progenitors of steroidogenic lineages. *Proceedings of the National Academy of*  
483 *Sciences of the United States of America*. 2009;106(50):21185-90.

484

## Figure Legends

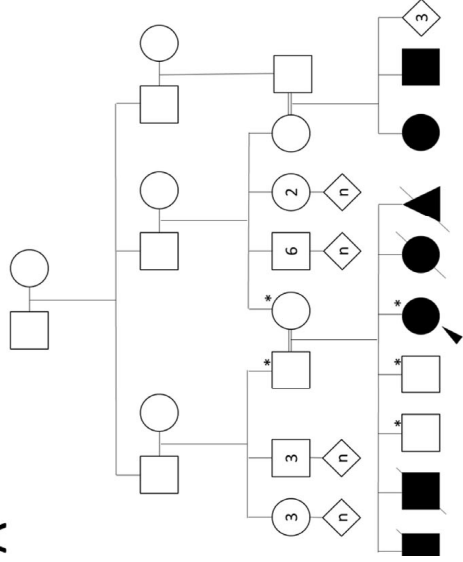
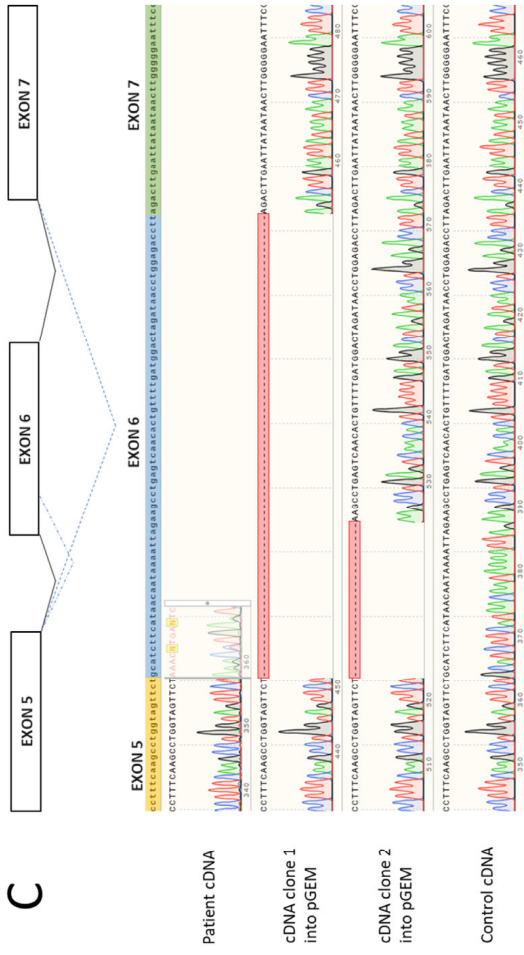
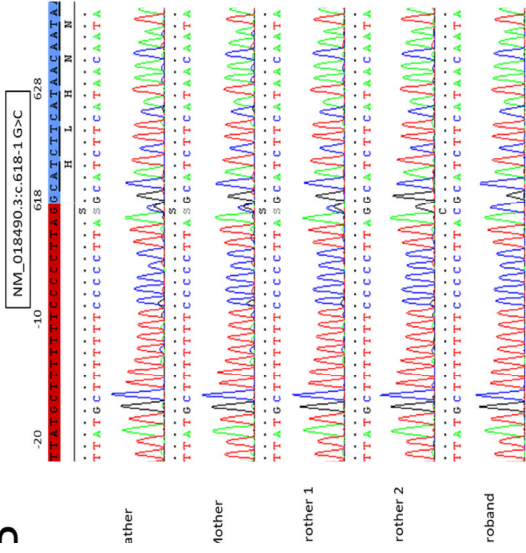
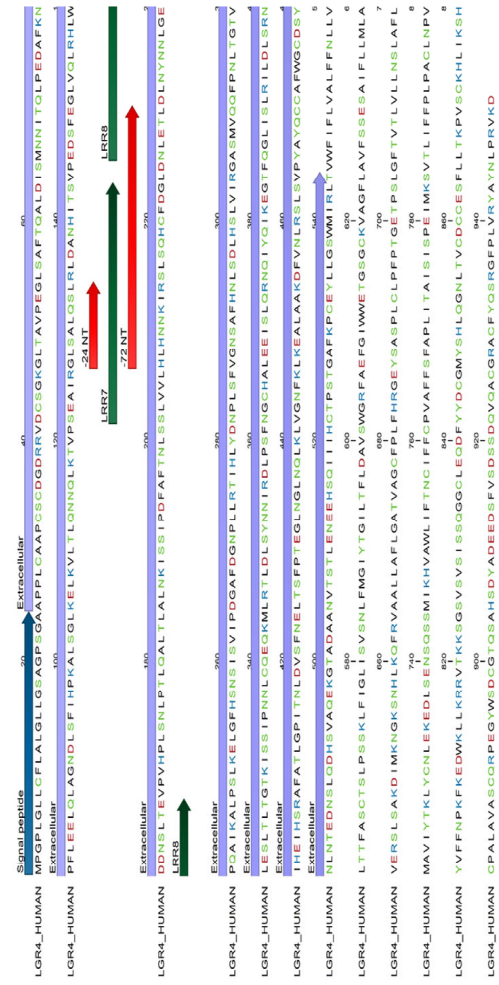
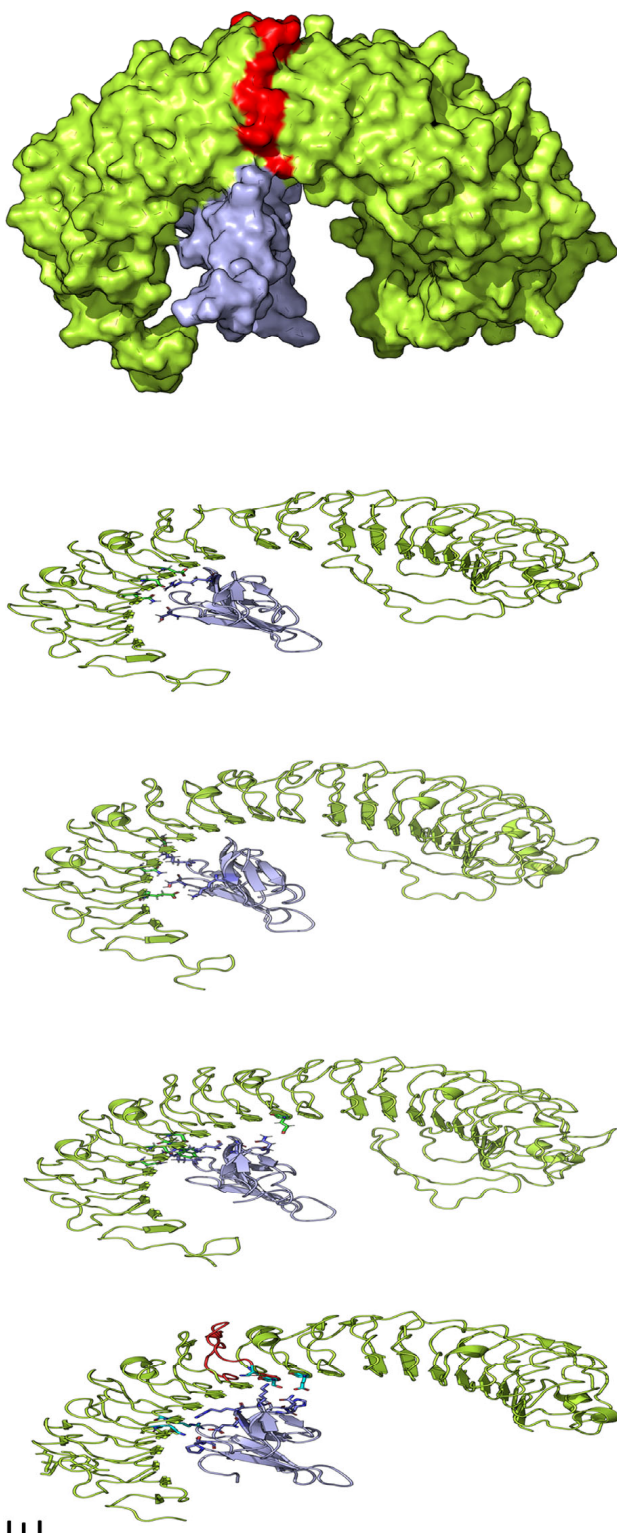
**Figure 1. Genetic and structural characterization of a novel human *LGR4* mutation identified in a highly consanguineous family.** **A.** Family pedigree showing first-degree consanguinity and multiple affected individuals. Squares, circles, and diamonds indicate male, female, unknown sex family members, respectively. Triangle indicates a miscarriage. Black symbols represent affected individuals and clear symbols unaffected individuals. Numbers in the symbol indicate multiple individuals. The black arrow indicates the index patient. Asterisk indicates individuals for whom DNA was sequenced. **B.** Partial chromatograms showing the identified *LGR4* mutation at NM\_018490.5:c.618-1 G>C. The reference sequences of intron 5 and exon 6 are highlighted in red and blue, respectively. The proband's parents and one of the brothers are heterozygous, one brother revealed the wild-type sequence, while the proband is homozygous. **C.** *LGR4* mRNA analysis from fibroblast tissue of the proband. The reference sequences of exons 5, 6, and 7 are highlighted in yellow, blue and green, respectively. The first track represents the patient mRNA after reverse transcription indicating the presence of two transcripts. The two transcripts were separated by cloning and sequenced; results are shown in the two-middle tracks. The bottom track represents the sequencing of the cDNA of control fibroblasts. The scheme above indicates normal splicing in dark lines and the impact of the mutation on the splicing in blue dotted lines. **D.** Amino acid sequence of human *LGR4* and showing the extracellular domain of *LGR4* that binds to RSPO proteins. Amino acids deleted by mutations found in the patient are located in LRR7 (-8 AA) and LRR7/8 (-24) AA coded by exon 6 of *LGR4*. **E.** Structural analysis of *LGR4* and its interaction with RSPO proteins. From left to right: 1) Structure of human *LGR4* extracellular domain in complex with part of RSPO1 (PDB 4KT1). Amino acids coded by exon 6 are depicted in red. 2) Complex of human *LGR4* with human RSPO3. The RSPO3 shares high structural similarity to RSPO1 and binds to *LGR4* in similar manner, interacting with LRR7 and 8 of *LGR4*. 3 and 4) models of *LGR4*

from the patient with missing 8 or 24 amino acids in LGR4. Several critical hydrogen bonding residues in LGR4 are missing due to mutations causing weaker interaction and binding of RSPO3 to mutant LGR4 proteins. 5) A surface view of the LGR4-RSPO3 complex, showing the close interaction points and the amino acids coded by exon 6 are shown in red.

**Figure 2. Protein expression and functional testing of the two LGR4 variants on Wnt/ $\beta$ -catenine signaling.** Human fibroblasts and HEK cells were used. **A.** Western blot analysis for LGR4 protein expression in patient and control fibroblasts. A representative blot of 3 independent experiments is shown. B-actin was used as a loading control. The molecular weight (kDa) of a protein standard is given. **B.** RSPO1 activated, LGR4 mediated Wnt signaling in HEK293 cells. Cells were transfected with wild-type (WT) or mutant LGR4 mt -24 and mt -72 plasmids (including a mock control) and reporter vectors TOP-Flash and Renilla. Signaling was stimulated by RSPO1 and assessed by the Dual-Luciferase assay (Promega). Results are expressed as relative LUC activities (RLU). Mean and SD of 3 independent experiments is shown. Student's t-test, \*  $P < 0.01$ . **C, D.** Interaction of RSPO1 with membrane-localized wild-type and variant LGR4. HEK293 cells were transfected with HA-tagged LGR4 plasmids (pcDNA3 LGR4wt, mt-24bp, mt-72bp) and incubated with conditioned RSPO1-GFP SN medium (previously produced in HEK cells transfected with pSpark- RSPO1-GFP). Cells were fixed with *Carnoy's* solution. Staining was with first antibody anti HA-Tag (green), second antibody anti-mouse Alexa 594 (red). Immunofluorescent microscopy was used to detect the cellular distribution of the tagged proteins as well as their colocalization (Zeiss LSM 710). Three independent experiments were analyzed. Representative pictures of confocal analysis at magnifications 40x are shown for wild-type and variants of LGR4. Scale bars show 5 and 10  $\mu\text{m}$ , respectively. Quantification of colocalized LGR4 and RSPO1 was performed by Imaris (Bitplane AG, Zürich, Switzerland).

**Figure 3. *Lgr4* ablation disrupts Wnt/ $\beta$ -catenin signaling pathway resulting in adrenal hypoplasia and aberrant zonal differentiation.** A. RT-qPCR analysis of mRNA encoding Wnt/ $\beta$ -catenin signaling pathway associated genes. B. Immunohistochemical detection of  $\beta$ -catenin and Lef1. C. LEF1-positive cells index defined as the percentage of LEF1+ cells over the total number of cortical cells. D. Adrenal weight. E. Hematoxylin and Eosin staining of wild type and *Lgr4*cKO adrenals. F. Number of cortical cells per 500  $\mu\text{m}^2$  of the cortex. G. Co-immunostaining for *Akr1b7* and *Dab2* in wild type and *Lgr4*cKO adrenals. H. RT-qPCR analysis of mRNA encoding zone-specific markers (*Akr1b7*, *Dab2* and *Hsd3b6*). All analyses were conducted in 5 weeks wild-type and *Lgr4*cKO female mice. zF: zona fasciculata, zG: zona glomerulosa, M: medulla, Co : cortex. Scale bars, 50  $\mu\text{m}$ . Bars represent the mean expression  $\pm$  SEM. Numbers of individual samples analysed are indicated within the bars. Statistical analyses in panels A, C, D, F & H were conducted using Mann-Whitney tests in GraphPad Prism 9. ns, not significant \* $P < 0.05$ , \*\* $P < 0.01$ , \*\*\* $P < 0.001$ , \*\*\*\* $P < 0.0001$ .

**Figure 4. *Lgr4* ablation inhibits zG differentiation, resulting in primary hypoaldosteronism.** A. Aldosterone plasma concentration and B. Renin activity in 5 weeks wild type and *Lgr4*cKO female mice. C. Immunohistochemical detection of CYP11B2 (scale bars 50  $\mu\text{m}$ ). D. Number of CYP11B2-positive cells per adrenal section. E. Corticosterone and F. Plasma ACTH concentration. G. RT-qPCR analysis of mRNA encoding steroidogenesis-related genes. All analyses were conducted in 5 weeks wild-type and *Lgr4*cKO female mice. Bars represent the mean expression  $\pm$  SEM. Numbers of individual samples analysed are indicated within the bars. Statistical analyses in panels A, B, D, E, F & G were conducted using Mann-Whitney tests in GraphPad Prism 9. ns, not significant \* $P < 0.05$ , \*\* $P < 0.01$ .

**A****C****B****D****E**

1

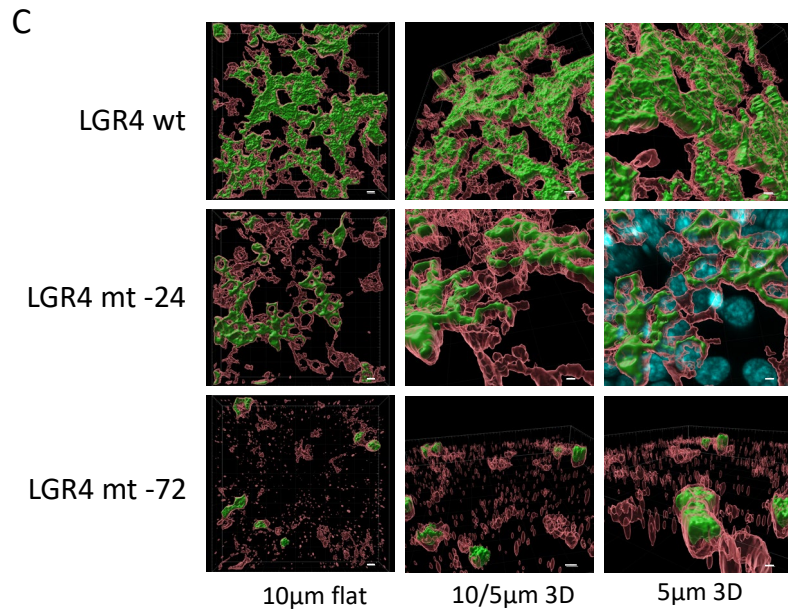
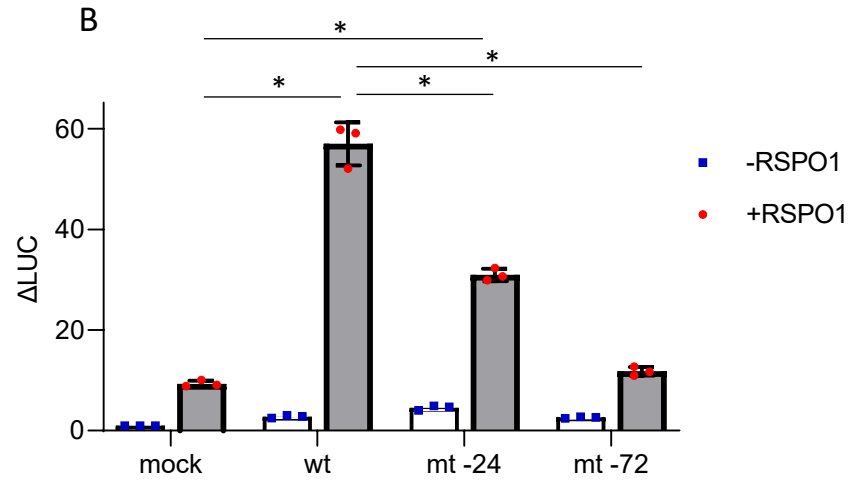
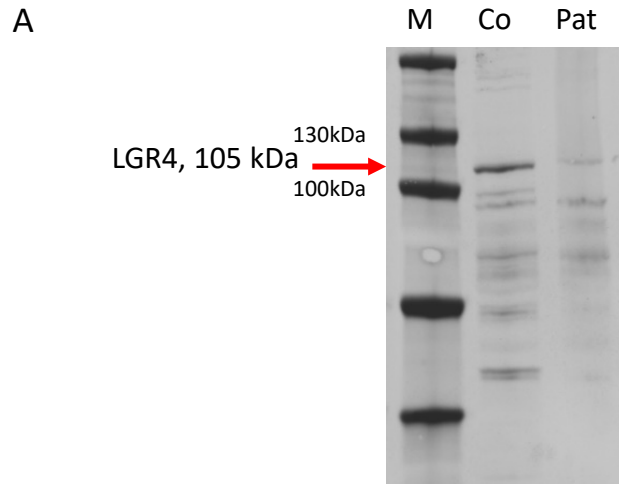
2

3

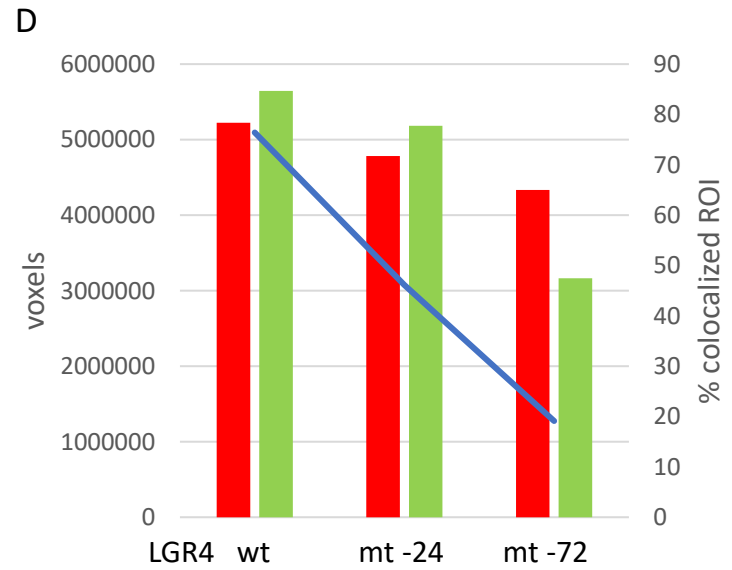
4

5

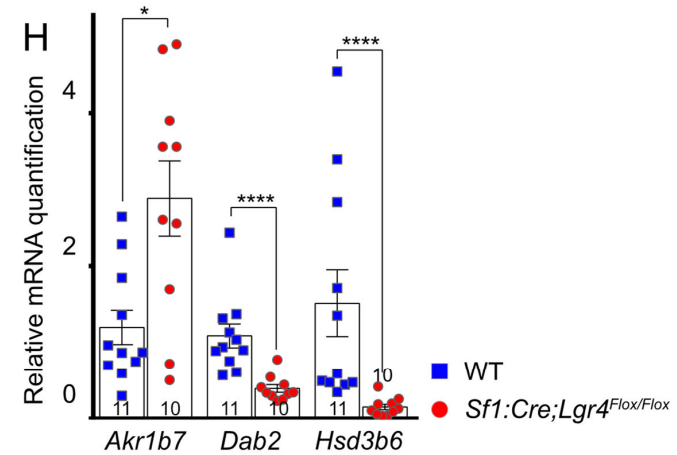
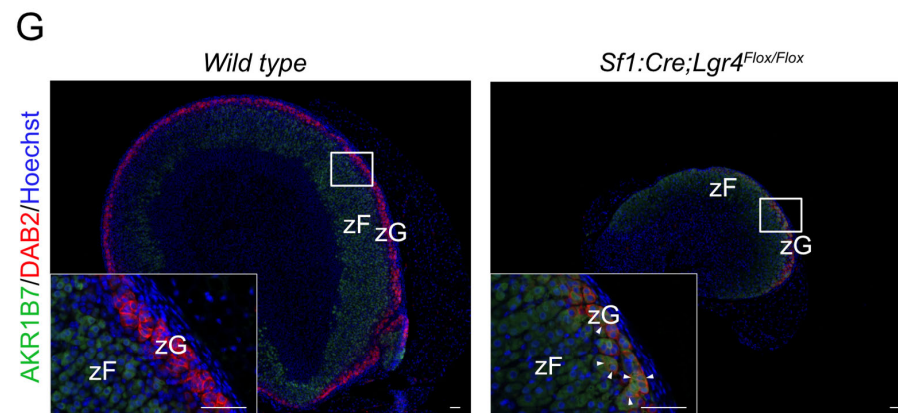
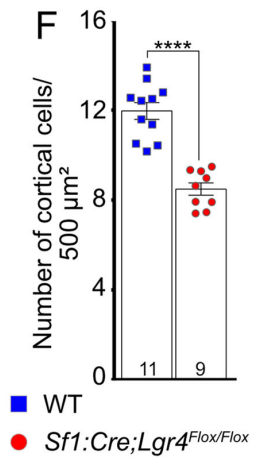
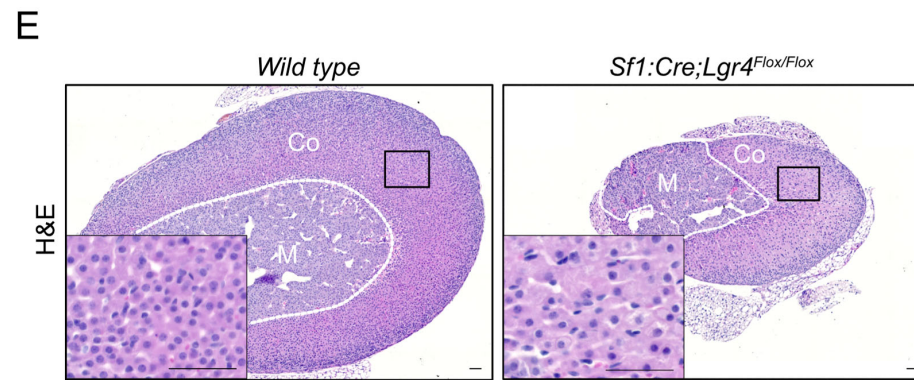
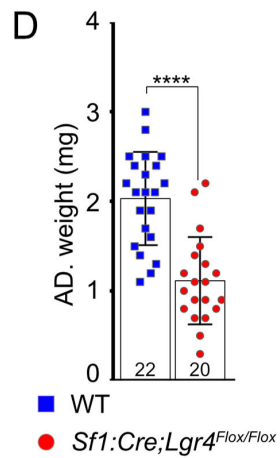
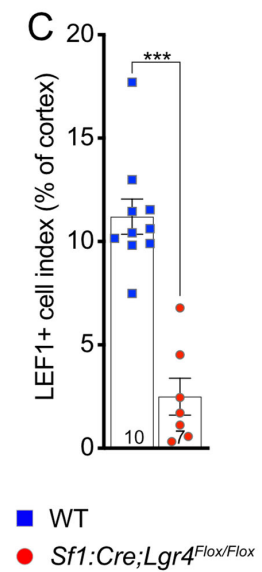
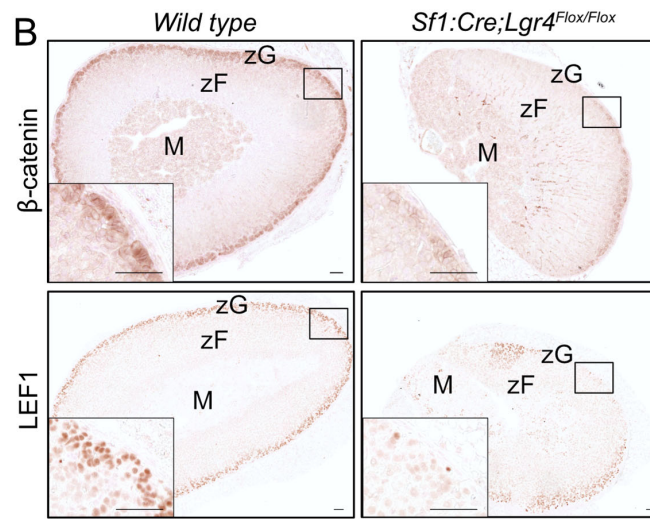
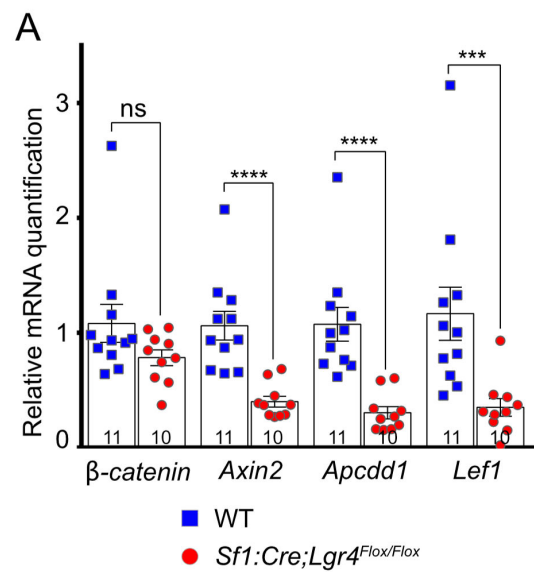




red: LGR4-HA, Alexa 546; green: RSP01-GFP







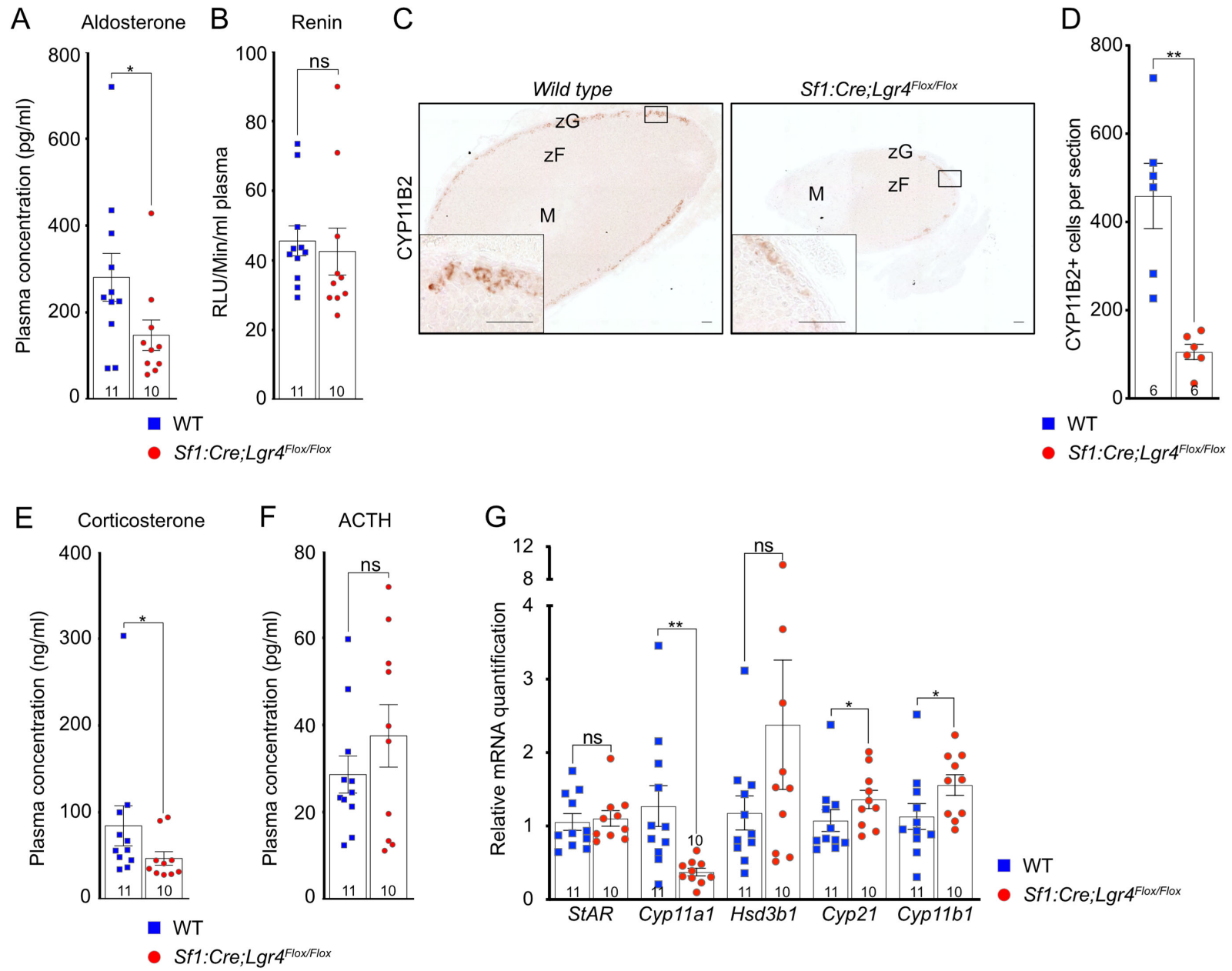


**Table 1. Patient characteristics and laboratory findings at initial presentation and during 4 years follow-up**

Age	years		17	17 1/3	17 1/3	18	20	21	21
Height	cm			141		142	142	142	
Weight	kg			33.5		36.1	34.7	36.4	
BMI	kg/m <sup>2</sup>					17.9	17.2	18.05	
Blood pressure	mmHg			103/74		113/76	127/85	116/80	
Pubertal stage	Tanner			4-5		5	5	5	
Bone age	years GP			16-17		adult			
Hydrocortisone	mg/m <sup>2</sup> /d		23.9	24h off treatment	0	0	0	0	
Florinef	ug/d		150	24h off treatment	0	100	100	24h off treatment	
		<b>Normal range basal</b>	<b>basal</b>	<b>basal</b>	<b>ACTH stimulated</b>	<b>basal</b>	<b>basal</b>	<b>basal</b>	<b>ACTH stimulated</b>
Na	mmol/l			136		138	137	142	
K				4.2		4.5	3.8	3.7	
Cl				106		108	106	110	
Creat	umol/l			79		72	69	64	
ACTH	ng/l	7.2-63.3	9.3	47.8		8	6.1	44.3	
Renin	ng/l (*mU/L)	1.7-23.9 (*4.4-46)	<b>38</b>	<b>133</b>		<b>*187</b>	20.8	9.1	
Corticosterone	nmol/l	1.69-63.8						1.08	9.91
Aldosterone	pmol/l	87-662	<b>41</b>	<b>nd</b>		<b>49.2</b>		<b>nd</b>	<b>nd</b>
17OHProg	nmol/l	0.24-6.84	4.2	<b>16.6</b>	20.2	3	1.5	<b>8.26</b>	15.7
Progesterone	nmol/l			20.5	15.6	3		42.1	
Cortisol	nmol/l	133-537		400	564	288.7	205	206	<b>303</b>
DHEA-S	umol/l	1.77-9.99	3.7	4.35	4.55	2.3	2.4	3.79	3.29

<b>DHEA</b>	<i>nmol/l</i>	1.7-38.3		8.2	9			7.93	11.3
<b>Androstendione</b>	<i>nmol/l</i>	1.06-7.72	8.5	<b>13</b>	15.9	3.4	3.3	6.89	7.45
<b>Testosteron</b>	<i>nmol/l</i>	0.31-2.29						1.33	1.54
<b>E2</b>	<i>pmol/l</i>	45-854	151	903			475	1264	
<b>LH</b>	<i>U/l</i>		11.8	17.7			12.2	5.7	
<b>FSH</b>	<i>U/l</i>		4.7	3.2			4.6	1.3	
<b>AMH</b>	<i>pmol/l</i>	7.14-57.1		13.3				22.4	
<b>IGF-1</b>	<i>ng/ml</i>		170	205			207		
<b>IGF-BP3</b>	<i>mg/l</i>		4.26	5.16			3.5		
<b>iPTH</b>	<i>pg/ml</i>	15-65						29.3	
<b>25OHVitD3</b>	<i>nmol/l</i>	50-135						60	
<b>Osteocalcin</b>	<i>ng/ml</i>	11-43						34.3	
<b>b-Cross-Laps</b>	<i>pg/ml</i>	<573						357	
<b>totP1NP</b>	<i>ng/ml</i>	15.1-58.6						<b>84.3</b>	
<b>FGF23</b>	<i>pg/ml</i>	10-50						50.7	

Footnotes: nd, not detected; numbers in bold mark findings outside the normative range